Liquid Crystals
Publication details, including instructions for authors and subscription information:
http://www.informaworld.com/smpp/title~content=t713926090

Structural investigations on B_7 phases of new bent-core mesogens including a binary system

G. Pelzl[a]; S. Diele[a]; M. W. Schröder[a]; W. Weissflog[a]; M. G. Tamba[a]; U. Baumeister[a]
[a] Martin-Luther-Universität Halle-Wittenberg, Institut für Physikalische Chemie, Halle, Germany

Online publication date: 06 July 2010

To cite this Article Pelzl, G. , Diele, S. , Schröder, M. W. , Weissflog, W. , Tamba, M. G. and Baumeister, U.(2010) 'Structural investigations on B_7 phases of new bent-core mesogens including a binary system', Liquid Crystals, 37: 6, 839 — 852
To link to this Article: DOI: 10.1080/02678292.2010.488019
URL: http://dx.doi.org/10.1080/02678292.2010.488019

Liquid Crystals,
Vol. 37, Nos. 6–7, June–July 2010, 839–852

Taylor & Francis
Taylor & Francis Group

INVITED ARTICLE

Structural investigations on B_7 phases of new bent-core mesogens including a binary system

G. Pelzl*, S. Diele, M.W. Schröder, W. Weissflog, M.G. Tamba and U. Baumeister

Martin-Luther-Universität Halle-Wittenberg, Institut für Physikalische Chemie, Halle, Germany

(*Received 27 November 2009; accepted 10 December 2009*)

Twelve new five-ring bent-core compounds have been synthesised which are derived from 2-nitroresorcinol and which contain only ester linkage groups. Their mesophase behaviour was investigated by polarising microscopy, X-ray diffraction and electro-optical measurements. It was found that most of the compounds studied form a B_7 phase. For several compounds, a phase transition between a B_7 high-temperature phase (B_{7H}) and a B_7 low-temperature phase (B_{7L}) was clearly detected by calorimetry, by a small change of the texture and by X-ray diffraction measurements. For one compound, (**A12**), well-aligned samples were obtained which allowed a more detailed structural characterisation of the B_7 phases. Interestingly, by fast cooling of the isotropic liquid, the same compound forms a metastable columnar phase. Furthermore, the binary system composed of the compound **A12** and a member of the B_7 parent series was investigated. X-ray diffraction measurements give evidence that the B_7 phases of both mixing components are completely miscible, i.e. they belong to the same phase type.

Keywords: bent-core mesogens; B_7 phases; X-ray diffraction; binary system

1. Alfred Saupe's relation to the liquid crystal research in Halle

It may be said that Alfred Saupe's scientific career has one of its roots in Halle. The story dates back to the 1930s when Wilhelm Kast was appointed as Professor of Physics at the University of Halle. He continued the research on liquid crystals that Daniel Vorländer had started in Halle in 1900. Together with Wilhelm Kast his graduate student, Wilhelm Maier, came to Halle, who gained both his thesis and his habilitation in the field of liquid crystals.

In 1946, after World War II, Wilhelm Maier left Halle and continued his scientific work on liquid crystals in Freiburg (Breisgau), and under his leadership his graduate student, Alfred Saupe, wrote a diploma thesis about ultraviolet (UV) spectroscopy in nematic liquid crystals in 1955, and in 1958 a doctoral thesis which was the basis of the famous Maier–Saupe theory.

It should be emphasised that at the beginning of the 1960s there was a close relationship between Wilhelm Maier in Freiburg and Horst Sackmann in Halle, who had published the first papers about the classification of smectic liquid crystals at the end of the 1950s. Wilhelm Maier visited the Halle LC group in 1963, and in 1965 Alfed Saupe also came to Halle and gave a lecture about nuclear magnetic resonance (NMR) studies in nematic solvents (a topic which was also the subject of his habilitation in 1967).

In 1970 the Second International Liquid Crystal Conference took place in West Berlin. The political situation in the former German Democratic Republic (GDR) prevented the participation of scientists from East Germany at the conference. In order to make contact in spite of this situation, an illegal meeting was arranged at the zoo in East Berlin at the time of the conference. Alfred Saupe and his wife came to East Berlin in order to meet members of the Halle group (Dietrich Demus and Gerhard Pelzl). Even that was not so easy. While Brigitte Saupe could pass through the border without any problems Alfred Saupe was held up for 2 hours because the conference material he carried with him (in English and including mysterious Greek symbols) looked very suspicious. Only after a number of phone calls did it became clear to the border guards that the public security of the GDR was not endangered, and finally Alfred Saupe could also pass across the border. At the zoo in East Berlin Alfred Saupe reported about the conference and handed over the extensive conference material. The younger member of the Halle group (G.P.) had the opportunity to discuss with Alfred Saupe a lot of scientific problems concerning his thesis, which was very helpful for him. Alfred Saupe's next visits to the University of Halle took place in 1986, during the Liquid Crystal Conference of Socialist Countries, and in 1990, on the occasion of his stay at the Science College in West Berlin. In 1992, after his retirement, Alfred Saupe came to Halle for nearly 5 years; he became the leader of a liquid crystal research group of the Max Planck Society, which was established in the Institute of Physical Chemistry and which closely co-operated with the liquid crystal group of

*Corresponding author. Email: g.g.pelzl@t-online.de

ISSN 0267-8292 print/ISSN 1366-5855 online

DOI: 10.1080/02678292.2010.488019
http://www.informaworld.com

this Institute. In this way, the scientific transfer took place in the reverse direction, from Alfred Saupe to Halle, so that the circle was closed again.

Discussions with Alfred Saupe about scientific problems were always useful because he was competent in theoretical questions as well as in practical experiments. We remember him as a patient listener who quickly got to the core of a problem. Everyone benefited greatly from these discussions, which were always very stimulating. Alfred Saupe was an unpretentious and modest scientist who did not make a great fuss about his person. All of us have to thank Alfred Saupe for his support during the difficult times after the Berlin Wall came down.

In the context of this paper it should be noted that the fascinating properties of the B_7 phase had attracted Alfred Saupe's strong interest and gave rise to many discussions. Alfred Saupe was also a co-author of one of the first publications which dealt with the nucleation of the B_7 phase [1].

2. Introduction

Bent-core mesogens have gained considerable importance because they are able to form new mesophases with unusual physical properties. Due to their bent shape the molecules within the smectic layers can be tightly packed in the bend direction, which leads to a long-range correlation of the lateral dipoles and to a polar axis [2]. Depending on the polar order in adjacent layers, switchable ferroelectric or antiferroelectric phases can occur. Another aspect of fundamental interest is the combination of polar order and director tilt, which causes the chirality of smectic layers although the constituent molecules are achiral [3, 4]. This property can be regarded as a supramolecular chirality. Depending on the structural features of the bent molecules, a mismatch of the space required by the rigid cores and the flexible terminal chains, and special polar forces, can give rise to a frustration of the layered structure that leads to undulated smectic phases or to columnar phases of different structure in which the columns are represented by polar layer fragments [5–10].

Among the mesophases formed by bent-core compounds the B_7 phase has attracted special attention because of an unusual nucleation on cooling the isotropic liquid and the formation of complex and beautiful optical textures [11, 12]. This mesophase was first reported for five-ring bent-core compounds prepared from 2-nitroresorcinol, here also named as the parent series. It grows like screw-like and telephone wire germs or beaded filaments. Simultaneously, striped focal conics, checkerboard textures, banana leaf-like and circular domains can arise [11, 12]. As shown by Jakli *et al.* [1], the screw-like nuclei consist of smectic filaments which form single, double or triple coils. The X-ray pattern of a powder-like sample displays a diffuse wide-angle scattering, indicating a liquid-like lateral order of the molecules. Furthermore, several sharp reflections in the small-angle region and a reflection in the medium-angle region occur, which point to a 2D or 3D superstructure. Interestingly, nearly simultaneously with the first description of the B_7 phase in 1999 another banana phase was reported which showed a quite similar nucleation and similar textures but possessed an undulated layer structure with an undulation period between 15 and 70 nm [13]. This phase later designated as B_7' [6] exhibits, in contrast to the B_7 phase, in most cases a polar switching using moderate electric fields. According to Coleman *et al.*, the structural feature of the B_7 and B_7' phase is a splay of polarisation which avoids a macroscopic polar order and which gives rise to the undulation of the smectic layers (B_7') or to two-dimensionally and three-dimensionally, respectively, ordered layer fragments (B_7) [14, 15]. Caused by the splay polarisation, two types of characteristic defect walls can appear, those where the chirality and clinicity changes between neighbouring stripes and those where the clinicity changes and the chirality remains.

In this paper different aspects of the B_7 phases are studied and discussed on the basis of results obtained on new homologous five-ring bent-core compounds. These compounds are derived from 2-nitroresorcinol and contain only ester linkage groups, in contrast to the parent series of the B_7 phase. It will be shown that the dependence on the length of the terminal chains causes a slight modification of the B_7 structure, whereas the introduction of lateral substituents at the outer phenyl rings has no significant influence on the structural features of the B_7 phase. For some of the compounds studied, a phase transition within the region of the B_7 phase could be clearly detected. Furthermore, we found for one homologue of the series that depending on the cooling rate from the isotropic liquid different structures, meaning different phases, occur which could be analysed by X-ray diffraction on aligned samples.

In order to compare the structure of the B_7 phase in our new series with that of the parent series we have also investigated a binary system between members of these two series.

3. Materials

The compounds, **An** and **AnX** (see Scheme 1), have been prepared by esterification of 2-nitroresorcinol with the corresponding 4-(4-n-alkyloxybenzoyloxy)-benzoic acids and 4-(4-n-alkyloxy-3-halogeno-benzoyloxy)benzoic acids, respectively, by means of dicyclohexylcarbodiimide using catalytic amounts of dimethylaminopyridine in dichloromethane as a solvent. The crystallisation from a mixture of ethanol and

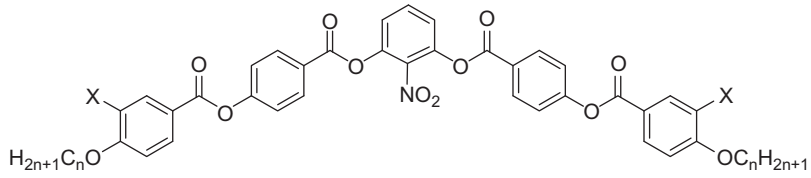

Scheme 1. General formula of the new compounds **An** and **AnX** (X: F, Cl, Br).

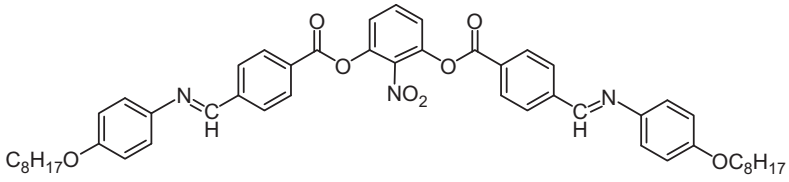

Scheme 2. **MC1** Cr 116 B_{7L} 122 B_{7H} 177 Is.

dimethylformamide resulted in pure materials, with yields of about 41–68%.

The mixing component **MC1** exhibiting a B_7 phase is the octyloxy homologue of the B_7 parent series [5, 12, 16] (see Scheme 2).

4. Experimental

The phase transition temperatures were determined with a differential scanning calorimeter (Pyris1, Perkin Elmer) and a polarising microscope (DMRXP, Leica) equipped with a hot stage HT80 and an automatic temperature controller (Mettler-Toledo). The assignment of the mesophases was mainly based on X-ray diffraction studies. Measurements were carried out on powder-like samples in glass capillaries kept in a temperature-controlled heating stage using a Guinier film camera or a Guinier goniometer (Huber Diffraktionstechnik GmbH) and quartz-monochromatised CuKα radiation. In cases when surface aligned fibre-like disordered samples could be obtained by slowly cooling a drop of the isotropic liquid placed on a glass plate on a temperature-controlled heating stage, 2D diffraction patterns have been recorded using Ni-filtred CuKα radiation and an area detector (HI-Star, Siemens/Bruker). Electro-optical measurements were performed using commercial ITO cells (EHC Corp.) of 5 or 6 μm thickness.

5. Results

5.1 The homologous series A8-A16

X-ray diffraction measurements show that the homologues with comparatively short terminal chains (**A8, A9**) do not exhibit liquid-crystalline phases. The decyloxy homologue **A10** forms a highly viscous phase which shows a non-specific texture with oval domains on cooling the isotropic liquid. A powder-like sample displays a diffuse X-ray scattering in the wide-angle region and sharp reflections at small and medium angles. The small-angle reflections have been further analysed by the X-ray patterns of a partially aligned sample (see Figure 1) and could be indexed on an oblique 2D lattice with the parameters $a = 60.8$ Å, $b = 38.0$ Å, $\gamma = 107.3°$ (at 120°C). A little broadened reflection in the medium angle range at $2\theta = 11.8°$, $d = 7.53$ Å (at 120°C) was also observed for the B_7 phase of the parent series. These data can be interpreted as shown below for those of compound **A12**.

The samples of the homologue **A11** also could not be aligned for X-ray measurements but the Guinier powder pattern was found to be quite similar to that of compound **A10.** Since the texture of compound **A11**, shown in Figure 2, is strongly reminiscent of that observed for compound **A10**, again, we can assume that both compounds form the same mesophase.

The dodecyloxy homologue **A12** is the most interesting member of the homologous series. First, depending on the experimental conditions (cooling rate, surface conditions, sample thickness) a complex texture is observed on cooling the isotropic liquid. On slow cooling of the isotropic liquid a mainly low-birefringent texture appears which displays screw-like nuclei, striped focal conics, checkerboard domains, and banana leaf-like domains characteristic of a B_7 phase (see Figure 3).

At 120°C a phase transition within the mesophase region was detected by a small calorimetric peak (see Table 1) which is also indicated by a slight but reproducible change of the texture in some areas of the sample. During this transition the birefringence changes a little, and furthermore, the stripes existing in some focal conic areas disappear and a smoother texture results, see Figure 4. Therefore we will distinguish between a low (L) and high (H) temperature

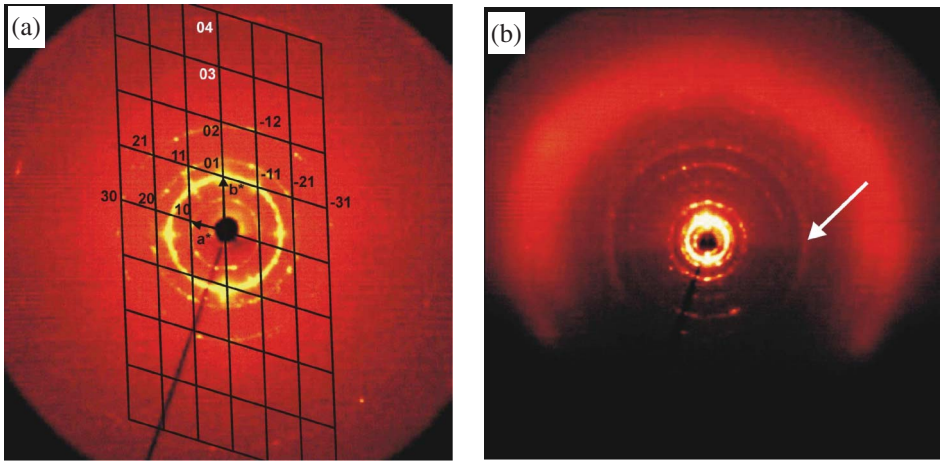

Figure 1. 2D X-ray patterns for a partially surface-aligned sample of **A10** at 120°C on cooling: (a) small-angle region showing axes and indexing for an oblique 2D lattice, (b) wide-angle pattern showing the diffuse outer scattering and the broadened reflection in the medium-angle range (arrow).

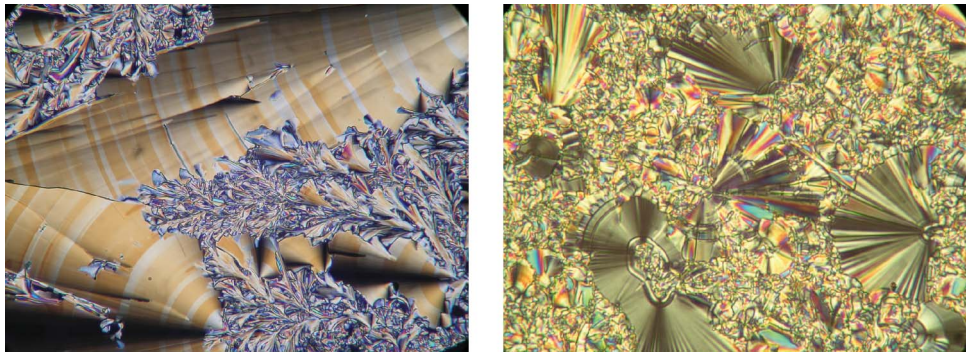

Figure 2. Microscopic texture of the B_7 phase of compound **A11** at 118°C.

form of the B_7 phase (B_{7L} and B_{7H}). The same phase transition was also found for the homologues **A14** and **A16** with longer terminal chains (see Table 1).

For electric fields above 15 V/μm optical switching could be observed leading to a clear increase in birefringence, but the extinction crosses of the circular or oval domains did not change. On removal of the applied field the birefringence again decreased and no changes in the position of the extinction crosses took place. Furthermore, the field-induced textures do not depend on the polarity of the field. Optical switching was also observed in the low-temperature phase, B_{7L}. In contrast to the measurements in the high-temperature phase, B_{7H}, a broad repolarisation peak was recorded on applying an AC field. A short-time experiment revealed two small repolarisation peaks. Unfortunately, in both B_7 phases long-time observations and the registration of the current response were prevented by the relatively high conductivity of the material and the rapid breakdown of the cell.

Since we were able to obtain quite well-aligned samples of compound **A12** on a glass plate we could study the structural features of its mesophases in more detail. The X-ray pattern recorded on *slow cooling* (up to about 5 K/min) is shown in Figure 5 (a)–(c). The diffuse part of the outer scattering with its maximum at 4.6 Å proves the liquid-like lateral order of the molecules. The small-angle reflections can be explained by a mesophase built up from layer fragments (columns) two-dimensionally ordered in an oblique lattice (see Figure 5(d)) with parameters $a = 62.5$ Å, $b = 41.4$ Å, $\gamma = 106°$ (122°C). An average tilt of the molecules with respect to the normal to a of $\tau = 27.5°$ is derived from the position of the maxima for the outer diffuse scattering (see packing models in Figure 5(f)). The apparent effective molecular length L_{eff} calculated from $d_{01} = 39.8$ Å and the tilt angle amounts to 44.9 Å using the relation $L_{eff} = d / \cos \tau$. This is a rather short value considering possible molecular lengths measured from molecular models for several chain conformations, varying between about 45 Å for a strongly bent overall shape

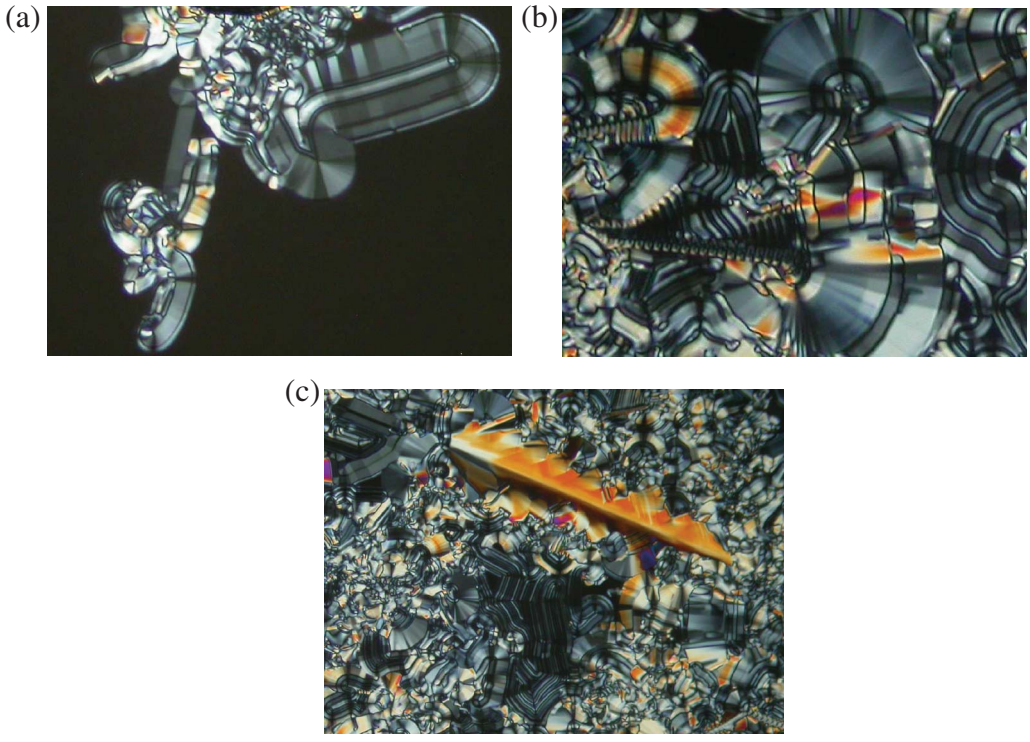

Figure 3. Compound **A12**; (a) nucleation of the B_{7H} phase at 126°C; (b, c) textures of the B_{7H} phase at 122°C; sample thickness 5 μm (colour version online).

Table 1. Transition temperatures (°C) and transition enthalpies (kJ/mol) of the 2-nitroresorcinol derivatives **An** and **AnX**.

No.	n	X	Mesophase behaviour
A8	8	H	CrI 128.0 [a)] CrII 132.7 [64.9a)] I
A9	9	H	CrI 117.7 [36.7] CrII 130.3 [33.8] I
A10	10	H	CrI 105.1 [37.6] CrII 125.0 [27.3] (B_7 119.3 [26.8])b) I
A11	11	H	CrI 89.9 [32.4] CrII 125.8 [27.9] (B_7 120.3 [27.3]) I
A12	12	H	Cr 118.5 [34.3] B_{7L} 120.3 [0.5] B_{7H} 126.8 [29.4] I
A14	14	H	Cr 114.2 [36.3] B_{7L} 119.3 [0.9] B_{7H} 128.4 [29.3] I
A16	16	H	Cr 114.8 [46.2] (B_{7L} 109.5 [0.5]) B_{7H} 129.5 [28.4] I
A12F	12	F	CrI 109.0 [32.5] CrII 129.8 [8.7] B_7 138.4 [31.3] I
A12Cl	12	Cl	Cr 139.9 [77.5] (B_7 130.9 [30.5]) I
A12Br	12	Br	Cr 132.1 [79.5] (B_7 126.5 [32.6]) I
A16F	16	F	CrI 103.8 [31.7] CrII 122.9 [12.0] B_{7L} 132.1 [1.0] B_{7H} 140.0 [31.5] I
A16Cl	16	Cl	Cr 116.8 [45.9] B_7 137.3 [31.2] I

Notes: Cr: crystalline phase, B_7: B_7 phase, B_{7H}: B_7 high-temperature phase, B_{7L}: B_7 low-temperature phase, I: isotropic liquid.
a) Both peaks are not sufficiently separated in the differential scanning calorimetry scan.
b) Monotropic transition values (in brackets) taken from the first cooling run.

and 63 Å for the most stretched one (see Figures 5(g), (h)). The streaks parallel to the meridian with a comparatively sharp maximum at $d = 7.4$ Å on the equator (see Figure 5(e)) are explained by a long-range ordered stacking of the molecules along the axes of the columns. These axes are the axes of polarisation and are aligned normal to the *a–b* plane. Due to the fibre-like disorder of the domains around the normal of the *a*-axis the period of 7.4 Å could be detected on the equator of the pattern. If we assume such a stacking, the significantly longer value compared with the average for the liquid-like distributed distances assumed for classic columnar bent-core phases of 5.2 Å (this value results for molecules with a bend angle of 120° with an average lateral distance between the molecules of 4.5 Å assuming a stacking in the bend direction) may be caused by the space additionally required by the NO_2 groups. There are two possibilities for how the rest of the molecule can adapt to this

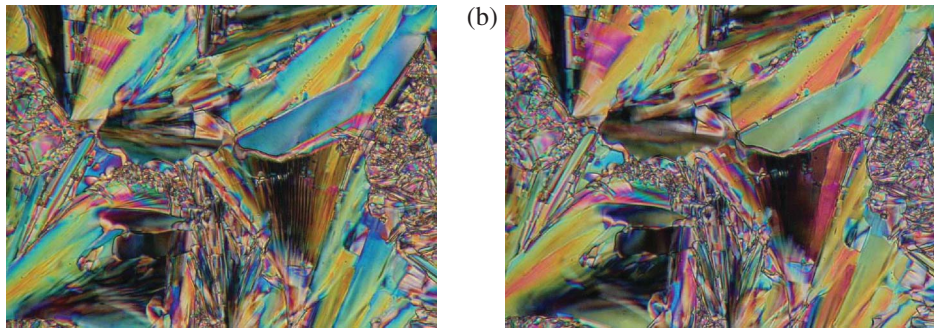

Figure 4. Compound **A12**; (a) texture of the B_{7H} phase at 121 °C; (b) texture of the B_{7L} phase at 118°C (colour version online).

expansion; by a partial intercalation or by a stronger bend. Figure 5(i) presents a sketch of the latter mode. We were not able to prove unambiguously the phase transition at 120°C by a discontinuous change of the X-ray pattern. However, on further cooling, the maxima on the streaks parallel to the meridian become more distinct and intense, i.e. the inter-columnar correlations become stronger, whereas the parameters for the 2D lattice change only slightly (cf. Table 2). An additional result is connected with the phase transition. The outer diffuse scattering becomes more and more asymmetric and shows two maxima in the theta-scans in the low-temperature phase (see Figure 12(a)), indicating two preferred maxima in the distribution of the lateral distances between the molecules. At about 70°C the outer diffuse scattering condenses to more or less sharp reflections, see Figure 5(c), and the lateral distances of the molecules adopt long-range order; the phase is now a true crystalline one with a rather high degree of disorder and/or very small crystallites.

A quite different X-ray pattern is obtained on *rapid cooling* of the isotropic liquid (cooling rate $>$ 10 K/min), see Figure 6. The small-angle reflections describe a two-dimensional rectangular lattice with parameters a = 51 Å and b = 75.3 Å. The reflection conditions (h_0 observed only for $h = 2n$ and $0l$ for $l = 2n$) imply the plane group $p2gg$ requiring an anticlinic arrangement for the molecules in adjacent (broken) layers (see Figure 6(d)). The directions of the maxima for the outer diffuse scattering reveal a tilt of the molecules with respect to b of about 35°, $d_{01}/\cos\tau$ amounts to 91.9 Å, which is approximately two times the effective molecular length estimated for the phase formed on slow cooling and fits with our model sketched in Figure 6(d). Hence we can assume that the molecular conformation is similar in both phases. There is *no* streak parallel to the meridian at medium angles, e.g. no hint of positional correlation between the molecules along the columnar axis as in the phase obtained on slow cooling.

We can assume that the phase with the oblique cell obtained on slow cooling is the stable one and the phase with the rectangular cell obtained on very fast cooling is the metastable phase. Interestingly, the Guinier film pattern recorded for a powder-like sample of **A12** in a glass capillary at about 122°C shows reflections of both, the oblique lattice and the rectangular lattice (see Table 2(a) and (c)) indicating the coexistence of a stable and a metastable phase.

Looking now at the longer-chained homologues **A14** and **A16,** the textures are quite similar to that of compound **A12**. They are less birefringent and show some ribbon-like domains, striped focal conics and circular domains with the extinction crosses parallel to the crossed polarisers. During the nucleation from the isotropic liquid, beaded filaments and many spiral germs having different structures appear (see Figure 7).

The optical switching of the homologues **A14** and **A16** was found to be quite similar to that of compound **A12**. In a short-time experiment we found two small repolarisation peaks for the high-temperature as well as for the low-temperature phase, which point to an antiferroelectric switching. The extinction crosses (parallel to the crossed polarisers) do not change on applying the electric field in the high-temperature phase, whereas a clockwise or anti-clockwise turn of the extinction crosses by about 30° is visible in the low-temperature phase, depending on the polarity of the applied field. On removal of the field the extinction crosses rotate again into the position parallel to the crossed polarisers. Unfortunately, also for these compounds the registration and analysis of the repolarisation peaks was impossible because of the relatively fast electric breakdown of the cells. These experimental findings indicate an antiferroelectric switching based on a collective rotation of the molecules around their long axes in the high-temperature phase. In the low-temperature phase the antiferroelectric switching

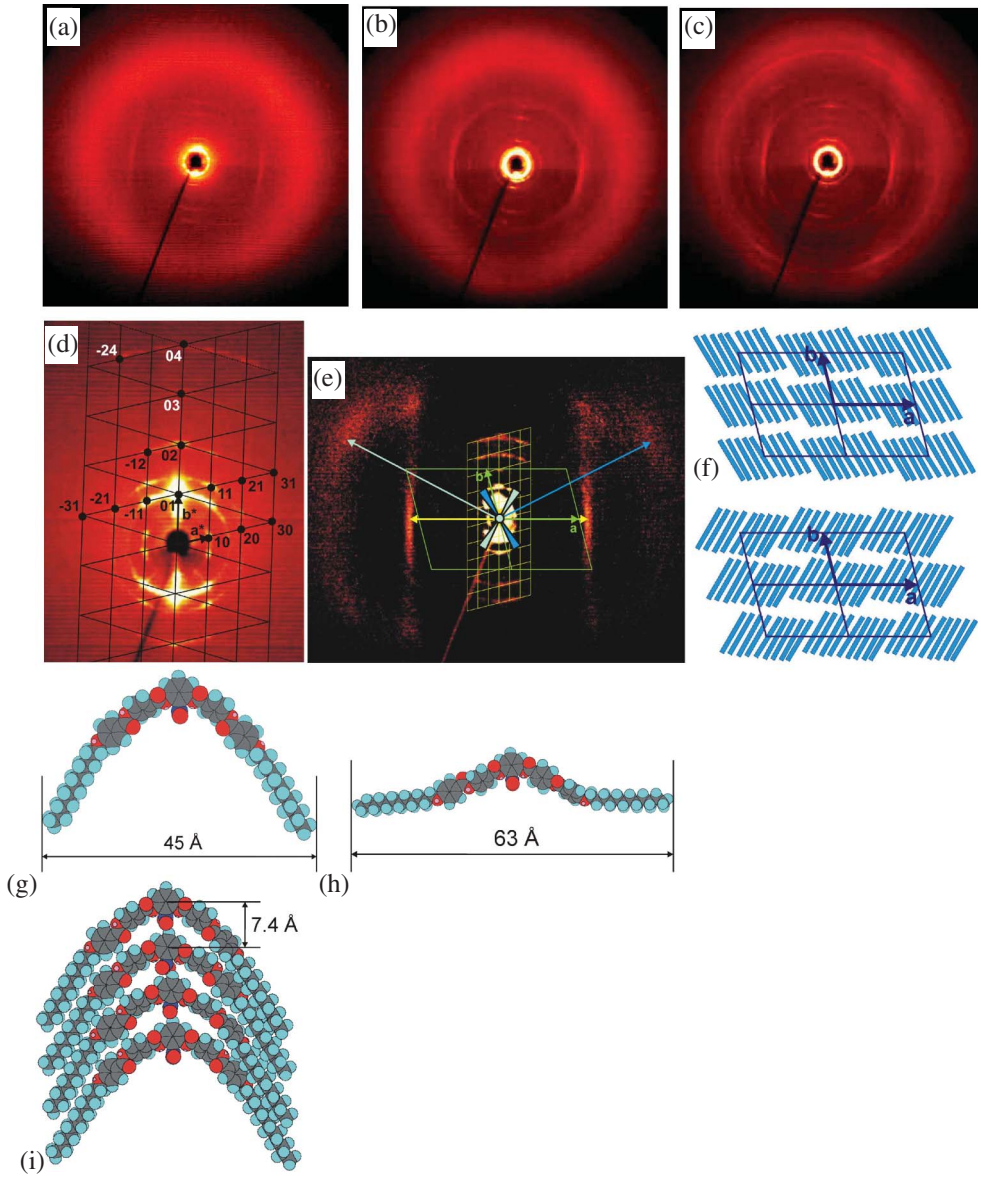

Figure 5. 2D X-ray diffraction patterns for a surface-aligned sample of **A12** on slow cooling: (a–c) original wide-angle patterns at 122°C (a), 115°C (b) and 70°C (c), (d) small-angle pattern at 122°C in the high-temperature phase showing the reciprocal 2D lattice for two orientations with indices for the observed Bragg reflections, (e) wide-angle pattern at 122°C (scattering of the isotropic liquid subtracted for better visibility of the maxima of the outer diffuse scattering) showing the mutual orientations of the reciprocal and real (with axes shown as green arrows) 2D lattices, the maxima of the streaks on the equator (yellow arrows), the maxima of the outer diffuse scattering (blue arrows) and the corresponding orientation of the molecules, (f) the two possible packing modes in the high-temperature phase, the polar (bent) directions are on average normal to the 2D lattice and cannot be determined from these X-ray measurements, (g–i) molecular models (Chem3D, CambridgeSoft.Com) for two extreme chain conformations with the molecular length, (g) strongly bent overall shape, (h) most stretched one, (i) tentative stacking of strongly bent molecules matching the model assumed from the X-ray data (stacking distance about 7.4 Å, molecular length about 45 Å).

obviously takes place by a collective rotation of the molecules around the tilt cone.

We could not obtain any aligned samples for the X-ray investigations on compounds with more than 12 carbon atoms in the chains. Nevertheless, the main features of the patterns for powder-like samples of **A14** and **A16** are the same as those for the short-chain homologues, a diffuse outer scattering at about 4.6 Å, Bragg reflections in the small-angle region which are not harmonics of each other, and one a little broadened reflection at medium angles with $d = 7.4$ Å in analogy to **A12** a Col_{obl} lattice with a periodic stacking along the axes of the columns which is found to be characteristic for the B_7 phase (see Figure 8).

Table 2. Data for the small-angle X-ray reflections of **A12** from surface-aligned (2D) and powder-like samples (one Guinier film pattern at 122°C): Indexing for (a) the high-temperature phase at 122°C on *slow cooling* on an oblique 2D lattice with parameters $a = 62.5$ Å, $b = 41.4$ Å, $\gamma = 106°$, (b) the low-temperature phase at 115 °C on *slow cooling* on an oblique 2D lattice with parameters $a = 61.0$ Å, $b = 41.4$ Å, $\gamma = 106°$, (c) the high-temperature phase at 122°C on *rapid cooling* on a rectangular 2D lattice with parameters $a = 51.0$ Å, $b = 75.3$ Å.

(a)	2D				Guinier	
hk	θ_{obs}/°	d_{obs}/Å	d_{calc}/Å	$(d_{obs} - d_{calc})$/Å	θ_{obs}/°	d_{obs}/Å
10	0.736	60.0	60.1	–0.1		
01	1.125	39.3	39.8	–0.5	1.125	39.3
–11	1.146	38.5	38.4	0.1		
20	1.474	30.0	30.0	0.0	1.463	30.2
11	1.492	29.6	29.6	0.0	1.508	29.3
–12	2.169	20.4	20.7	–0.3	2.157	20.4
02	2.236	19.8	19.9	–0.1		
03	3.350	13.2	13.3	–0.1		
–24	4.343	10.2	10.3	–0.1		
04	4.350	10.2	9.9	0.3		
05	5.451	8.1	8.0	0.1		

(b)	2D			
hk	θ_{obs}/°	d_{obs}/Å	d_{calc}/Å	$(d_{obs} - d_{calc})$/Å
10	0.758	58.2	58.6	–0.4
01	1.114	39.7	39.8	–0.1
–11	1.142	38.7	38.2	0.5
11	1.495	29.6	29.4	0.2
–21	1.629	27.1	27.5	–0.4
–12	2.159	20.5	20.7	–0.2
02	2.220	19.9	19.9	–0.0
03	3.346	13.2	13.3	–0.1
–14	4.319	10.2	10.3	–0.1
–24	4.333	10.2	10.3	–0.1
04	4.320	10.2	9.9	0.3
–25	5.386	8.2	8.3	–0.1

(c)	2D				Guinier	
hk	θ_{obs}/°	d_{obs}/Å	d_{calc}/Å	$(d_{obs} - d_{calc})$/Å	θ_{obs}/°	d_{obs}/Å
11	1.064	41.5	42.2	–0.7		
02	1.172	37.7	37.6	0.0	1.175	37.6
12	1.452	30.4	30.3	0.1	1.463	30.2
20	1.732	25.5	25.5	0.0	1.738	25.4
13	1.956	22.6	22.5	0.1	1.950	22.7
04	2.345	18.8	18.8	0.0		

Notes: *hk*, Miller indices; $\theta_{obs,}$ observed Bragg angle; $d_{obs,}$ *d* value calculated from the observed Bragg angle; d_{calc}, *d* value calculated from the lattice parameters.

A comparison of the diffraction patterns for homologues with 10, 12, 14 and 16 carbon atoms in the chains is given in Figure 9.

The compounds **AnX** bearing lateral substituents presented in Table 1 exhibit quite similar phase behaviour to the non-substituted compounds; however, the transition within the mesophase region cannot be observed in most cases. Surprisingly, the attachment of fluoro and chloro atoms, respectively, at the lateral 3-position of the outer rings increases the clearing temperatures by up to 11 K; compare **A12** with **A12F** and **A12Cl**, as well as **A16** with **A16F** and **A16Cl**. The mesophases show similar optical textures, however, with lower birefringence; this includes the nucleation from the isotropic liquid where beaded filaments and screw-like germs can be observed.

The X-ray patterns for powder-like samples in the mesophases of compounds **A12F** and **A12Cl** closely resemble those of the corresponding unsubstituted compound **A12** obtained on slow cooling, therefore the structure of the phases may be assumed to be the same. A similar observation was made comparing the

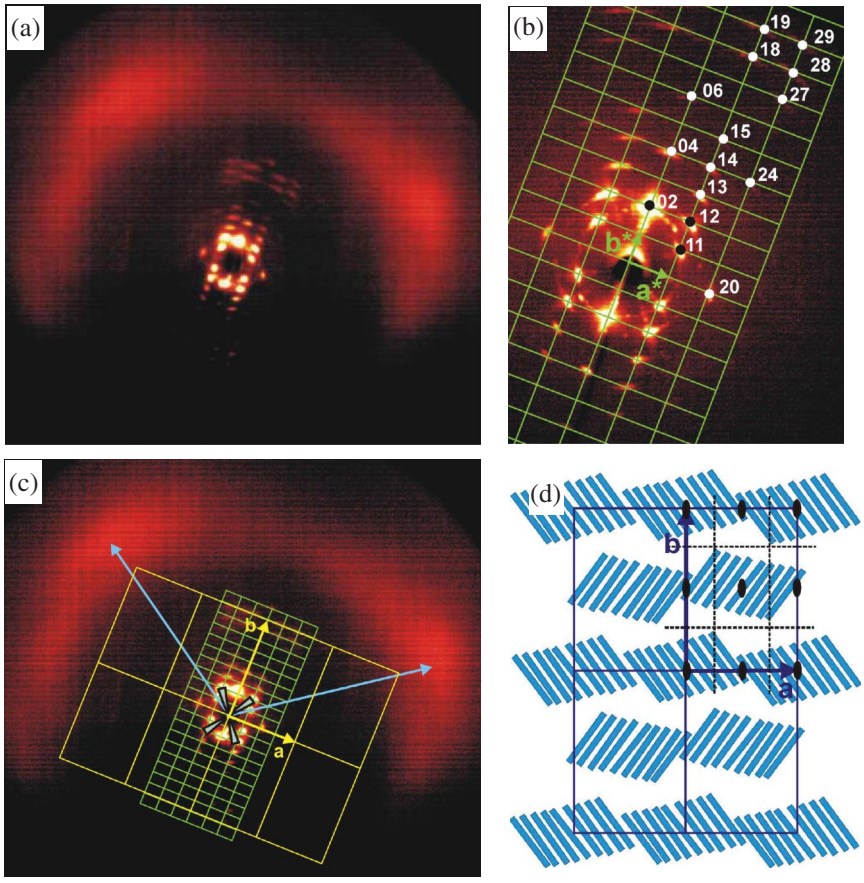

Figure 6. 2D X-ray diffraction patterns for a surface-aligned sample of **A12** at 122°C on rapid cooling: (a) original wide-angle pattern, (b) small-angle pattern showing the reciprocal 2D lattice with indices for the observed Bragg reflections in the asymmetric unit, (c) wide-angle pattern showing the mutual orientations of the reciprocal (shown as green lines) and real (yellow lines) 2D lattices, the maxima of the outer diffuse scattering (blue arrows) and the corresponding orientation of the molecules, (d) one of the possible packing modes with symmetry elements for plane group *p2gg* (polar directions cannot be determined from these X-ray measurements).

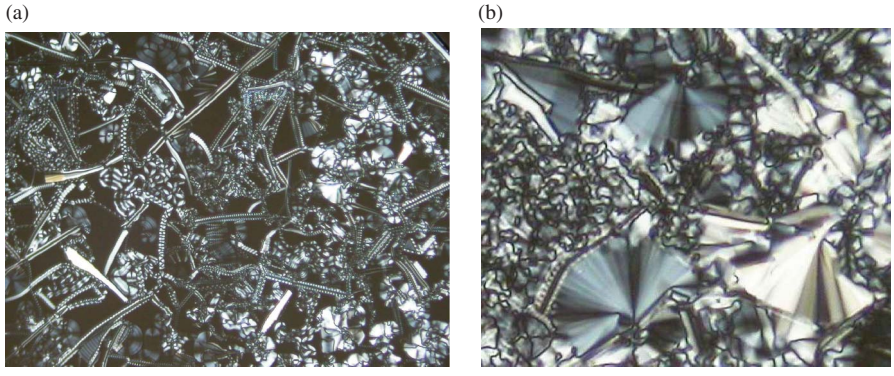

Figure 7. (a) Nucleation of the B_{7H} phase of compound **A14** at 126°C, sample thickness 5 μm, (b) texture of the B_{7H} phase at 120°C.

X-ray patterns in the mesophases of the halogenated long-chain homologues with the corresponding unsubstituted ones. As an example, Figure 10 shows a comparison for **A16** and **A16Cl**.

5.2 Miscibility studies

The assignment of the B_7 phase provides a general problem. A characterisation based only on texture observations, especially on the occurrence of helical

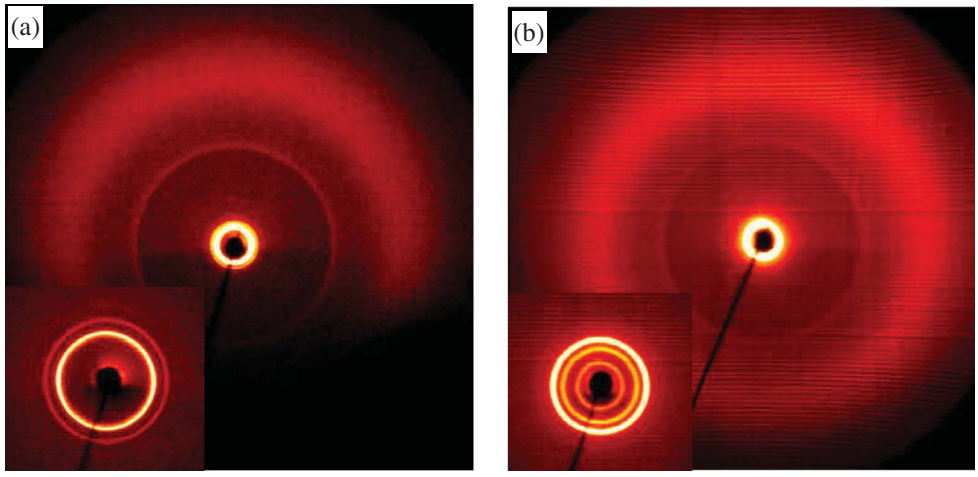

Figure 8. 2D X-ray patterns for powder samples of **A14** at 122°C (a) and **A16** at 126°C (b) on cooling (insets: small-angle patterns).

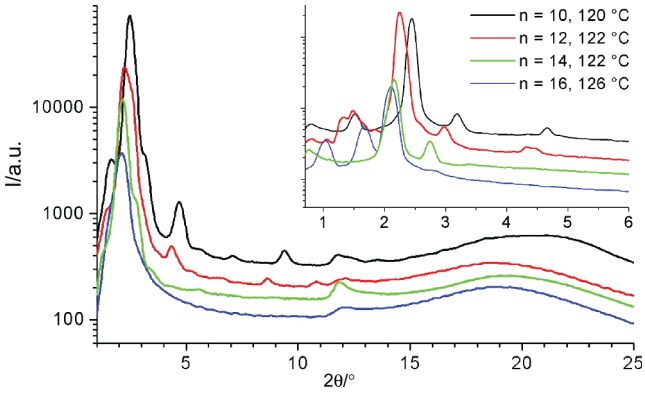

Figure 9. Theta-scans for the 2D X-ray patterns of **A10, 12, 14** and **16** on (slow) cooling (inset: small-angle region).

filaments, is very risky. The reason is that in some cases only non-specific textures occur. Moreover, the formation of helical filaments during the growing process is not an unambiguous criterion for a B_7 phase because these can also appear in smectic layer structures without molecular or supramolecular chirality [17–20]. The X-ray studies mostly suffer from the lack of well-oriented samples. For powder-like samples, often only the small-angle part of the pattern is considered and the closely neighboured reflections in the small-angle region prevent an unambiguous explanation of the structure by only one lattice. That is the situation, too, for the parent series with B_7 phases. In 2005, Folcia *et al.* [21] published detailed small-angle X-ray studies on non-oriented samples of the octyloxy homologue of this parent series (**MC1**, in our paper). They discussed four possible indexing models and, considering the relative intensity of the observed reflections with respect to that expected for the assumed symmetry, they proposed one model as the most probable.

We have re-investigated compound **MC1** with special attention focussed on the wide-angle scattering. In addition to the X-ray diagram reported elsewhere [12] we

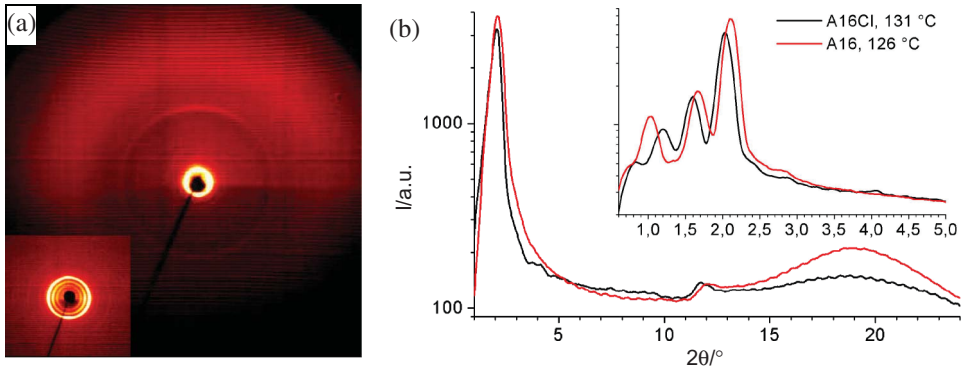

Figure 10. 2D X-ray patterns for a powder-like sample of **A16Cl** at 131°C (a) (inset: small-angle pattern), (b) theta-scans for these patterns (black lines) in comparison with those for **A16** (red lines), all on cooling.

found beside the reflection with $d = 7.5$ Å two maxima in the wide-angle scattering, which is assumed to be characteristic for the B_{7L} phase (see Figure 12(b)).

To overcome these problems, we have used miscibility studies, which have been a successful tool for the classification of liquid-crystalline phases of calamitic molecules. According to this well-established method, only phases with the same phase symbol (which implies the same symmetry) can form a region of an uninterrupted (complete) miscibility in a binary system [22].

5.3 The binary system A12/MC1

To answer the question of whether the mesophase of compound **A12** (the structure of which is now well-established, based on the X-ray studies of oriented samples) is structurally identical to the B_7 phase of the parent series, we investigated the binary system with compounds **A12** and **MC1.** Samples of five concentrations ($x_{\mathbf{A12}} = 0.25$; 0.50; 0.75; 0.85; 0.95) were prepared. We found that the textures of the mixtures are not identical, but exhibit some textural features as well as different helical nuclei during the growing process which are known for a B_7 phase. The X-ray patterns of powder-like samples were found to correspond best to those of compound **A12** recorded on slow cooling, in which the streaks at medium angles are clearly visible (see Figures 11 and 13). The shape of the outer diffuse scattering in the theta-scans (two maxima) speaks for the low-temperature modification B_{7L} (see Figure 12). The continuous development of the scattering angles of the main reflections with $x_{\mathbf{A12}}$ allowed us to index the patterns in agreement with those of compound **A12**, meaning by oblique 2D lattices with continuously changing lattice parameters as a function of concentration (see Figure 13, Table 3). The parameter a, corresponding to the width of the layer fragments in our model, decreases significantly from 105 Å for **MC1** to 61 Å for **A12**, i.e. the number of molecules laterally packed in these fragments becomes smaller. The parameter b changes only moderately between 36.8 and 41.4 Å, respectively, as well as the angle γ varying only slightly between 101° and 108°. There is no simple relation of these parameters to the molecular length, but the change of b seems to correspond to the change of the average molecular length from 40 Å for **MC1** (see Figure 14) to 45 Å for **A12** (see Figure 5(g)) in their strongly bent conformation. The possibility of this analogous indexing for the small-angle reflections (see Figure 13(a)), the same type of the diffuse outer scattering with two maxima, and the common, slightly broadened reflection at about 7.5 Å imply that the principal structure of the B_7 phase is the same. This means that the complete miscibility which was assumed by the texture observation could be clearly confirmed by the X-ray diffraction measurements.

6. Conclusions

As we have discussed, the assignment of the B_7 phases is problematic. In many cases, the B_7 phase was classified mainly because of the occurrence of different screw-like nuclei which are formed on slow cooling of the isotropic liquid. However, this is not an unambiguous criterion because any layer instability can lead to the formation of helical filaments during the growing process also in the absence of a molecular or layer chirality [17–20]. On the other hand, textural features which are obviously due to a splay of polarisation are a strong argument for the existence of a B_7 or B_7' phase.

The differentiation between the B_7 and the B_7' phases is an example of the case that phases can exhibit very similar and typical textures but different structures. According to X-ray studies, the B_7 phase possesses a columnar structure whereas the B_7' phase is characterised by an undulated layer structure. If B_7-typical textures occur in simple SmCP layer structures it can be assumed that the layer structure is also an undulated one but possesses a relatively large period (larger than 100 nm) which cannot be detected by

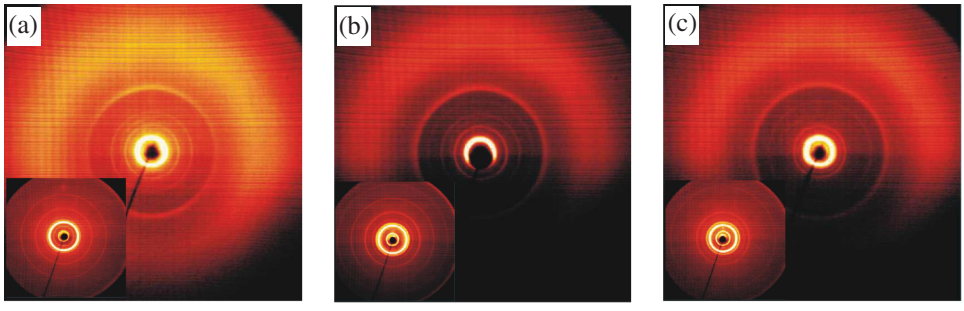

Figure 11. 2D X-ray patterns for powder-like samples of (a) **MC1** and two mixtures with (b) 0.25 mol% and (c) 0.75 mol% **A12** at 159°C, 128°C, and 129°C, respectively, on cooling (insets: small-angle patterns) (colour version online).

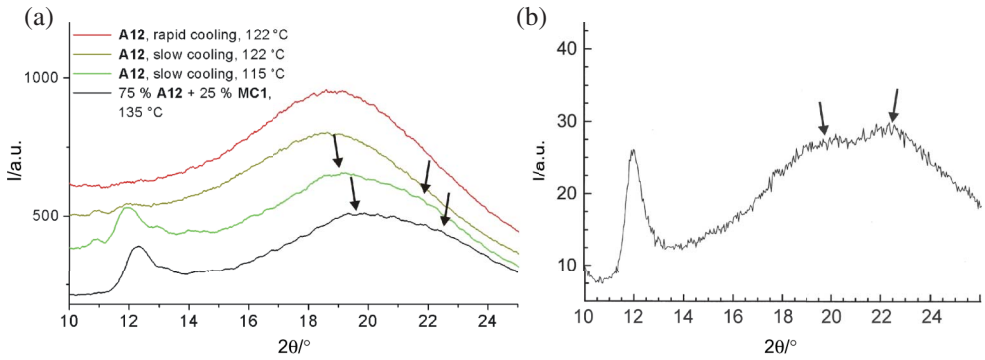

Figure 12. Theta-scans for the wide-angle X-ray patterns of (a) **A12** and a mixture with 75 mol% **A12** and (b) for **MC1** at 160°C.

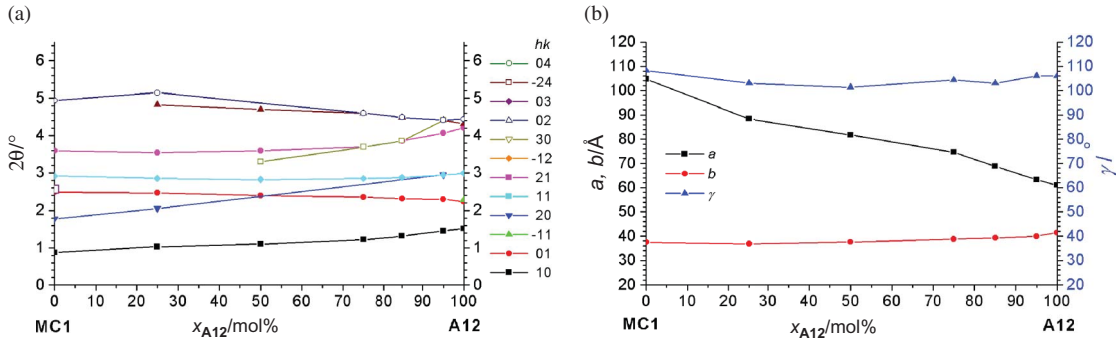

Figure 13. 2θ position of the observed small-angle reflections (a) and 2D lattice parameters (b) for the pure compounds and the mixtures of the binary system **A12** and **MC1** depending on x_{A12} based on an indexing in analogy to the pattern of the low-temperature phase formed by **A12** on slow cooling.

Table 3. 2D lattice parameters for the mixtures of the binary system **A12** and **MC1** depending on the composition of the mixture x_{A12} (mol %).

x_{A12}	T/°C	a/Å	b/Å	γ/°
0	159	104.7	37.5	108.2
25	128	88.4	36.8	103.0
50	138	81.8	37.6	101.3
75	129	74.6	38.8	104.3
85	123	68.8	39.3	103.0
95	120	63.3	40.0	106.0
100	115	61	41.4	106.0

Notes: T, temperature; a, b, γ, lattice parameters.

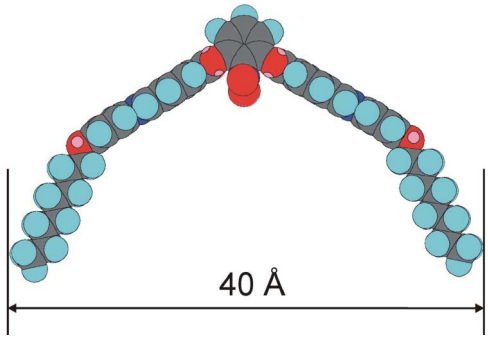

Figure 14. Molecular model (Chem3D, CambridgeSoft.Com) for **MC1** in its strongly bent overall shape with molecular length.

standard X-ray techniques. Concerning the phase classification on the basis of the texture, it must also be considered that sometimes only non-specific textures occur (as for the compounds **A10** and **A11**). Furthermore, for bent-core compounds with B_7–SmCP dimorphism, the B_7 phase adopts the texture of the SmCP phase which exists at higher temperatures [23–25]. In this case, X-ray measurements are the only possibility to decide if a B_7 phase is present or not.

The classification of a B_7 phase on the basis of X-ray diffraction measurements is also problematic. In most cases, the main problem is the lack of well-oriented samples. The assignment of two-dimensional indices to the very closely and non-equidistantly positioned small-angle reflections in the powder-like patterns is difficult, and can lead to different lattices for one and the same phase.

The compounds in the new homologous series **A** presented here form B_7 phases identical to those of the

parent series [11]. This statement is based on the pattern of a well-oriented sample of **A12**. The pattern allowed us an unambiguous assignment of the *hk*-indices to the observed reflections which led to an oblique lattice ($a = 62.5$ Å, $b = 41.4$ Å, $\gamma = 106°$). The structure is built up by columns of molecules in which the molecules are stacked with the bend direction normal to the *a*–*b* plane (Col_{ob}-structure). A characteristic reflection with a period of 7.4 Å found in all patterns of B_7 phases of different compounds points to a density modulation along the columns which can be explained by the distances of the molecules in the bend direction [25–30]. The form of the reflection in the pattern of oriented samples (a streak parallel to the meridian) proves the absence of strong correlations between the molecules of neighbouring stacks. From the position of the outer diffuse scattering, the average tilt angle of the molecules with respect to the normal of the *a*-axis could be measured to be $\tau = 27.5°$. Based on these experimental data a very small effective length of the constituent molecules is determined ($L_{eff} = 44.9$ Å). This means that the molecules must take on a strongly bent overall molecular shape.

Detailed texture observations point to a phase transition within the B_7 phase which is proved by a small but reproducible peak in the differential scanning calorimetry trace (0.5...1.0 kJ/mol) and minor but reproducible changes in the texture. A small but more continuous alteration also takes place in the X-ray patterns. The outer diffuse scattering splits into two diffuse maxima with decreasing temperature. In addition, maxima on the streaks parallel to the meridian become more distinct and intense, indicating an increasing correlation between the stacks of molecules. It may be speculated that one of the diffuse maxima is connected with lateral distances between the central parts of the aromatic bent core of the molecules, whereas the outer one is connected with the flexible chains. In this context it should be noted that Schmalfuss *et al.* [16] also reported a similar phase transition for the octyloxy homologue of the B_7 parent series (component **MC1**), which is indicated by a small calorimetric peak and by a discontinuous decrease of the dielectric permittivity.

Based on the results obtained for the homologue **A12** the X-ray patterns of the other homologues have been evaluated and their liquid crystalline phases could be designated as B_7.

Finally the structural agreement of the B_7 phase under discussion with those of the B_7 parent series has been proved by investigations of binary mixtures of compound **A12** with the octyloxy homologue **MC1** of the parent series. The continuous development of the pattern as a function of the concentration offered the possibility of evaluating the pattern in the same way as in the case of **A12**. By these comparative studies it was possible to generalise the structural peculiarities for the B_7 phase.

A very surprising result was the occurrence of the metastable Col_r phase of compound **A12**, which is formed by fast cooling of the isotropic liquid. In contrast to the stable Col_{obl} phase which appears on slow cooling, it does not exhibit streaks at medium angles which we now assume to be typical for the B_7 phase.

References

[1] Jakli, A.; Lischka, C.; Weissflog, W.; Pelzl, G.; Saupe, A. *Liq. Cryst*. **2000**, *27*, 1405–1409.

[2] Niori, T.; Sekine, T.; Watanabe, J.; Furukawa, T.; Takezoe, H. *J. Mater. Chem*. **1996**, *6*, 1213–1233.

[3] Link, D.R.; Natale, G.; Shao, R.; Maclennan, J.M.; Clark, N.A.; Körblova, E.; Walba, D.M. *Science* **1997**, *278*, 1924–1927.

[4] Brand, H.R.; Cladis, P.E.; Pleiner, H. *Eur. Phys. J. B* **2003**, *6*, 347–353.

[5] Pelzl, G.; Diele, S.; Weissflog, W. *Adv. Mater*. **1999**, *11*, 707–724.

[6] Amaranatha Reddy, R.; Tschierske, C. *J. Mater. Chem*. **2006**, *16*, 907–961.

[7] Ros, M.B.; Serrano, J.L.; de la Fuente, M.R.; Folcia, C.L. *J. Mater. Chem*. **2005**, *15*, 5093–5098.

[8] Takezoe, H.; Takanishi, Y. *Jpn. J. Appl. Phys*. **2006**, *45*, 597–625.

[9] Hird, H. *Liq. Cryst. Today* **2005**, *14*, 9–21.

[10] Mieczkowski, J.; Matraszek, J. *Polish J. Chem*. **2005**, *79*, 179–209.

[11] Pelzl, G.; Diele, S.; Jakli, A.; Weissflog, W. *Liq. Cryst*. **2006**, *33*, 1513–1518.

[12] Pelzl, G.; Diele, S.; Jakli, A.; Lischka, C.; Wirth, I.; Weissflog, W. *Liq. Cryst*. **1999**, *26*, 135–139.

[13] Lee, C.K.; Chien, L.C. *Liq. Cryst*. **1999**, *26*, 609–612; Lee, C.K.; Chien, L.C. *Ferroelectrics* **2000,** *243*, 231–239.

[14] Coleman, D.A.; Fensler, J.; Chattham, N.; Nakata, M.; Takanishi, T.; Körblova, E.; Link, D.L.; Shao, R.-F.; Jang, W.G.; Mondain-Monval, O.; Boyer, C.; Weissflog, W.; Pelzl, G.; Chien, L.C.; Zasadzinski, J.; Watanabe, J.; Walba, D.M.; Takezoe, H.; Clark, N.A. *Science* **2003**, *201*, 1204–1211.

[15] Coleman, D.A.; Jones, C.D.; Nakata, M.; Clark, N.; Walba, D.M.; Weissflog, W.; Fodor-Csorba, K.; Watanabe, J.; Novotna, V.; Hamplova, V. *Phys. Rev. E: Stat., Nonlinear, Soft Matter Phys.* **2008**, *77*, 021703-(1-6).

[16] Schmalfuss, H.; Hauser, A.; Kresse, H. *Mol. Cryst. Liq. Cryst*. **2000**, *351*, 221–228.

[17] Williams, C.E. *Philos. Mag*. **1975**, *32*, 313–321.

[18] Kleman, M.; Lavrentovich, O.D. *Soft Matter Physics: an Introduction*; Springer: New York, 2003.

[19] Tsafir, J.; Guedeau, M.-A.; Kandel, D.; Stavens, J. *Phys. Rev. E: Stat., Nonlinear, Soft Matter Phys.* **2001**, *63*, 031603-(1-11).

[20] Santangelo, C.D.; Pincus, P. *Phys. Rev. E: Stat., Nonlinear, Soft Matter Phys.* **2002**, *66*, 061501-(1-7).

[21] Folcia, C.L.; Etxebarria, J.; Ortega, J.; Ros, M.B. *Phys. Rev. E: Stat., Nonlinear, Soft Matter Phys.* **2005**, *72*, 041709-(1–5).

[22] Sackmann, H.; Demus, D. *Mol. Cryst. Liq. Cryst*. **1973**, *21*, 239–273.

[23] Pelzl, G.; Schröder, M.W.; Dunemann, U.; Diele, S.; Weissflog, W.; Jones, C.; Colemann, D.; Clark, N.A.; Stannarius, R.; Li, J.; Das, B.; Grande, S. *J. Mater. Chem*. **2004**, *14*, 2492–2498.
[24] Novotna, V.; Hamplova, V.; Kaspar, M.; Glogorova, M.; Knizek, K.; Diele, S.; Pelzl, G.; Jones, C.; Coleman, D.; Clark, N.A. *Liq. Cryst*. **2005**, *32*, 967–975.
[25] Amaranatha Reddy, R.; Sadashiva, B.K. *Liq. Cryst*. **2002**, *30*, 1365–1367.
[26] Shreenivasa Murthy, H.N.; Sadashiva, B.K. *Liq. Cryst*. **2003**, *30*, 1051–1055.
[27] Umadevi, S.; Sadashiva, B.K. *Chem. Mater.* **2006**, *18*, 5186–5192.
[28] Bedel, J.P.; Rouillon, J.C.; Marcerou, J.P.; Laguerre, M.; Nguyen, H.T.; Achard, M.F. *Liq. Cryst*. **2000**, *27*, 1411–1421.
[29] Shankar Rao, D.S.; Nair, G.G.; Krishna Prasad, S.; Anita Nagamani, S.; Yelamaggad, C.V. *Liq. Cryst*. **2001**, *28*, 1239–1243.
[30] Prasad, V. *Liq. Cryst*. **2001**, *28*, 1115–1120.